



New Amphiphilic Squalene Derivative Improves Metabolism of Adipocytes Differentiated From Diabetic Adipose-Derived Stem Cells and Prevents Excessive Lipogenesis

Munkhzul Ganbold¹, Farhana Ferdousi^{1,2}, Takashi Arimura¹, Kenichi Tominaga¹ and Hiroko Isoda^{1,2,3*}

¹ National Institute of Advanced Industrial Science and Technology (AIST)-University of Tsukuba Open Innovation Laboratory for Food and Medicinal Resource Engineering (FoodMed-OIL), Tsukuba, Ibaraki, Japan, ² Alliance for Research on the Mediterranean and North Africa (ARENA), University of Tsukuba, Tsukuba, Ibaraki, Japan, ³ Faculty of Life and Environmental Sciences, University of Tsukuba, Tsukuba, Ibaraki, Japan

OPEN ACCESS

Edited by:

Dariusz Widera,
University of Reading,
United Kingdom

Reviewed by:

Joseph Isaac Shapiro,
Marshall University, United States
Gianpaolo Papaccio,
Second University of Naples, Italy

*Correspondence:

Hiroko Isoda
isoda.hiroko.ga@u.tsukuba.ac.jp

Specialty section:

This article was submitted to
Stem Cell Research,
a section of the journal
*Frontiers in Cell and Developmental
Biology*

Received: 29 June 2020

Accepted: 14 October 2020

Published: 04 November 2020

Citation:

Ganbold M, Ferdousi F, Arimura T,
Tominaga K and Isoda H (2020) New
Amphiphilic Squalene Derivative
Improves Metabolism of Adipocytes
Differentiated From Diabetic
Adipose-Derived Stem Cells
and Prevents Excessive Lipogenesis.
Front. Cell Dev. Biol. 8:577259.
doi: 10.3389/fcell.2020.577259

Squalene (Sq) is a natural compound, found in various plant oils, algae, and larger quantity in deep-sea shark liver. It is also known as an intermediate of cholesterol synthesis in plants and animals including humans. Although evidences demonstrated its antioxidant, anticancer, hypolipidemic, and hepatoprotective and cardioprotective effects, its biological effects in cellular function might have been underestimated because of the water-insoluble property. To overcome this hydrophobicity, we synthesized new amphiphilic Sq derivative (HH-Sq). On the other hand, adipose-derived stem cells (ASCs) are a valuable source in regenerative medicine for its ease of accessibility and multilineage differentiation potential. Nevertheless, impaired cellular functions of ASCs derived from diabetic donor have still been debated controversially. In this study, we explored the effect of the HH-Sq in comparison to Sq on the adipocyte differentiation of ASCs obtained from subjects with type 2 diabetes. Gene expression profile by microarray analysis at 14 days of adipogenic differentiation revealed that HH-Sq induced more genes involved in intracellular signaling processes, whereas Sq activated more transmembrane receptor pathway-related genes. In addition, more important number of down-regulated and up-regulated genes by Sq and HH-Sq were not overlapped, suggesting the compounds might not only have difference in their chemical property but also potentially exert different biological effects. Both Sq and HH-Sq improved metabolism of adipocytes by enhancing genes associated with energy homeostasis and insulin sensitivity, *SIRT1*, *PRKAA2*, and *IRS1*. Interestingly, Sq increased significantly early adipogenic markers and lipogenic gene expression such as *PPARG*, *SREBF1*, and *CEBPA*, but not HH-Sq. As a consequence, smaller and fewer lipid droplet formation was observed in HH-Sq-treated adipocytes. Based on our

findings, we report that both Sq and HH-Sq improved adipocyte metabolism, but only HH-Sq prevented excessive lipogenesis without abrogating adipocyte differentiation. The beneficial effect of HH-Sq provides an importance of synthesized derivatives from a natural compound with therapeutic potentials in the application of cell therapies.

Keywords: squalene, derivative, ASC, diabetes, adipose-derived stem cell differentiation, adipocyte metabolism, adipocyte differentiation

INTRODUCTION

Human adipose-derived stem cells (ASCs) are adult stem cells obtainable by liposuction procedure. By definition, ASCs present high capacity to proliferate after isolation without losing their stemness, at the same time potential to differentiate into mesodermal cell lineages, including adipocytes, chondrocytes, osteocytes, and myocytes under appropriate inducing condition.

The therapeutic and regenerative effect of ASCs on insulin resistance, obesity, and type 2 diabetes (T2D)-associated complications has been investigated for a variety of purposes (Mazini et al., 2020). For example, multiple infusion of ASCs in diabetes-induced rats reversed diabetes-related complications and protected tissue damages by alleviating inflammation (Yu et al., 2019). A recent study revealed that subcutaneous transplantation of ASC sheet prepared from non-diabetic mice into diabetic mice improved glucose intolerance (Ishida et al., 2020). Subcutaneous injection and local administration of human adipose-derived stromal vascular fraction cells showed a beneficial effect on microcirculation in ischemic diabetic feet and wound healing (Nie et al., 2011; Moon et al., 2019). Moreover, its application in tissue engineering and fat grafting in reconstructive surgery is being extensively explored (Naderi et al., 2014, 2017).

However, previous studies raised questions about the effectiveness of ASCs isolated from a diabetic and obese donor on the clinical use of stem cells because of the predisposition of impaired biological functions and altered transcriptomes due to its microenvironment, thus diminishing its therapeutic value and further cellular function in the recipient. Proliferation, viability, and migration capacity of ASCs from the obese environment are reduced, and its transcriptome is altered and inflamed (Vyas et al., 2019).

Squalene (Sq), a polyunsaturated hydrocarbon, is found ubiquitously in numerous plant oils (Owen et al., 2000; He et al., 2002; Shimizu et al., 2019) and algae (Kaya et al., 2011) and also larger quantity in deep-sea shark liver (Hernández-Pérez et al., 1997). Sq is also synthesized in plants and animals including humans as an intermediate of sterol synthesis such as cholesterol. Knockout murine in which upstream enzyme of Sq synthesis was disrupted presented lipid dystrophy, hepatic steatosis, and severe diabetic abnormalities, showing its indispensable physiological function in the organism (Yeh et al., 2018). Numerous evidences demonstrated its antioxidant, anticancer, hypolipidemic, and hepatoprotective and cardioprotective effects. Dietary Sq supplement (1%) prevented colon carcinogenesis in rats (Rao et al., 1998); rabbits fed with Sq (3%) for 7 weeks unexpectedly showed no more atheroma

than the controls (Kritchevsky et al., 1953); moreover, in Sq feeding (900 mg/d) in human studies, serum triglyceride and cholesterol contents were unchanged (Strandberg et al., 1990). Interestingly, contrary to the expected, in the same studies, Sq feeding did not increase serum cholesterol level, whereas serum Sq level was augmented 17 times in humans after 30 days. These findings altogether suggest that Sq might be accumulated in the serum because of the lack of efficient absorption, even though its biological effect is beneficial.

Naturally, Sq is characterized as a hydrophobic lipid, and its biological properties in cellular function might have been underestimated because of the low solubility. Thus, to overcome this water-insoluble property, a recent study proposed a lysosome-embedded Sq structure and showed its preferential cytotoxic effect on LAN5 cancer cells in their preliminary study (Costa et al., 2018).

We have recently synthesized Sq derivative (HH-Sq) (Sasaki et al., 2020), which gained amphiphilic property compared to Sq. In this *in vitro* study, we explored the effect of HH-Sq compared to Sq on adipocyte differentiation of ASCs derived from diabetic donors to determine whether the gained hydrophilicity of the derivative can promote Sq's biological effects and eventually be used in therapeutic application.

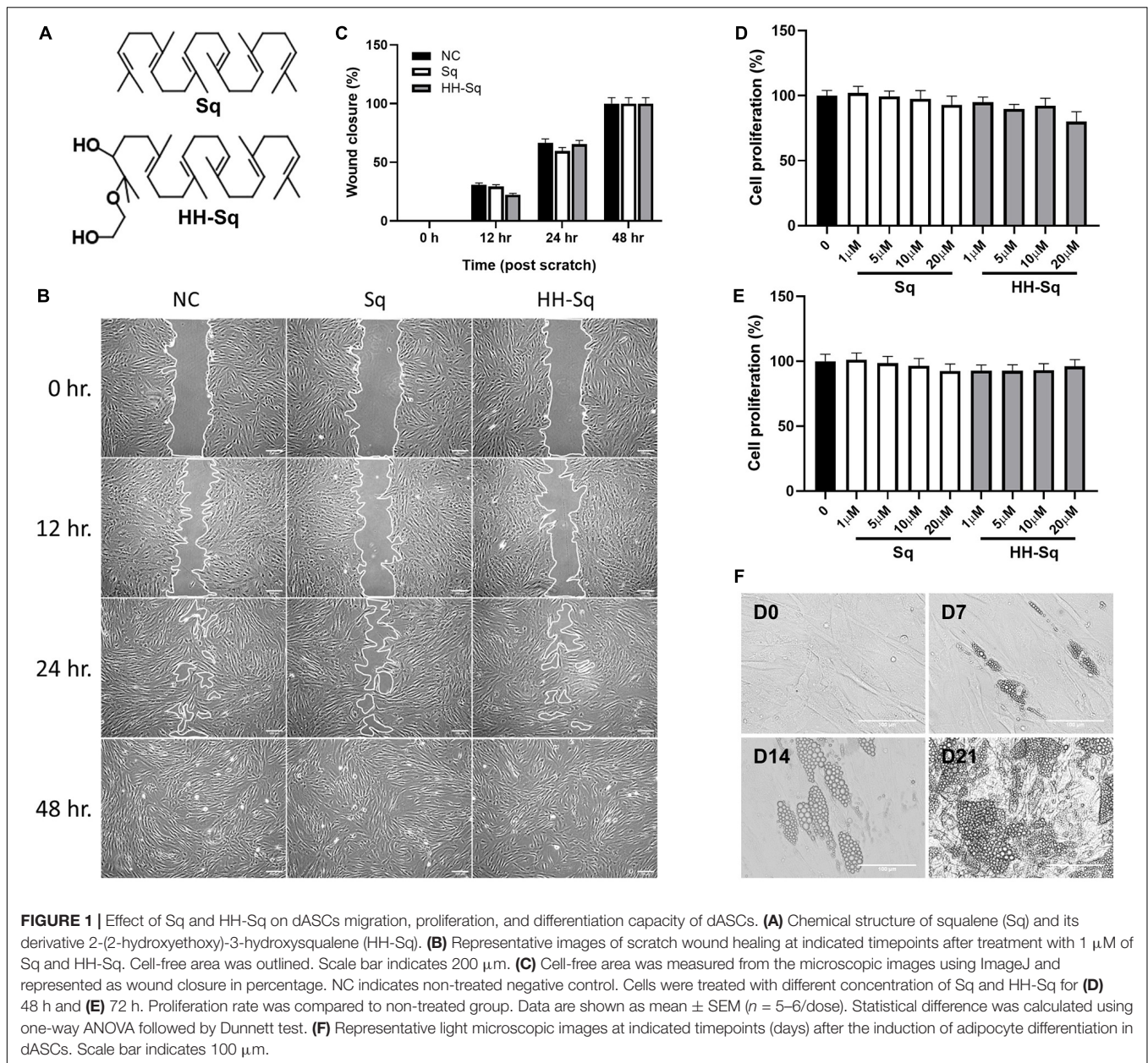
MATERIALS AND METHODS

Chemicals

Squalene was purchased from Fujifilm Wako (Tokyo, Japan). Sq mono ethylene glycol derivative, (2-(2-hydroxyethoxy)-3-hydroxysqualene) (HH-Sq), was synthesized as reported previously (Sasaki et al., 2020) and identified by spectral data (Figure 1A).

Adipose-Derived Stem Cells Culture

Diabetic ASCs (dASCs) (T2D; 74-year-old Caucasian woman, body mass index = 25 kg/m²) was purchased from Lonza (Walkersville, MD, United States; Material number: PT-5008, tissue acquisition number: 29752). These cells were isolated from donated human tissue after obtaining permission for their use in research only by informed consent or legal authorization. Cells were cultured in ASC growth medium (ADSC-GM BulletKit™) obtained from Lonza containing ASC basal medium supplemented with 10% fetal bovine serum, 1% L-glutamine, and gentamicin-amphotericin B (GA-1000) according to the manufacturer's instruction at 37°C in 5% CO₂ humidified incubator. Cells are subcultured 5,000 cells per cm² as recommended by the provider.



Adipogenic Differentiation of dASCs

Cells were seeded at a density of 3×10^4 cells per cm^2 in the preadipocyte growth medium (PGM-2TM BulletKit; Lonza, Walkersville, MD, United States). Once cells reach confluence greater than 80%, adipogenesis is induced by changing medium to adipogenic differentiation medium (ADM). According to the manufacturer's instruction, ADM was prepared by adding rhInsulin, dexamethasone, IBMX, and indomethacin into PGM. The medium was changed every 10 to 12 days.

Cell Proliferation Assay

Cell proliferation was determined using the CellTiter 96[®] AQueous One Solution Cell Proliferation Assay (Promega, Madison, WI, United States). Briefly, cells were seeded at

a density of 1×10^4 cells per well in 96-well plate for overnight and then treated with increasing concentration of Sq and HH-Sq. After 24 and 48 h of incubation, 20 μ L per well of CellTiter 96[®] AQueous One Solution Reagent was added and incubated for 3 h. Soluble formazan produced was measured by absorbance at 490 nm using a microplate reader (Varioskan LUX).

Cell Migration/Scratch Assay

Cells were grown in ADSC-GM until confluence in 6-well plate and then washed with phosphate-buffered saline (PBS) two times, scratched using a sterile 10 μ L micropipette tip, and incubated in ADSC-GM with treatment; the microscopic photo was taken at several timepoints; the cell-free area was measured using ImageJ.

Lipid Droplets Staining

Cells were seeded on a chamber slide, and adipogenesis differentiation was induced in the presence or absence of Sq and HH-Sq as described above. Lipid droplets (LDs) formed after differentiation were stained by fluorescent neutral lipid dye 4,4-difluoro-1,3,5,7,8-pentamethyl-4-bora-3a,4a-diaza-s-indacene (BODIPY 493/503; Invitrogen, Eugene, OR, United States), mounted with ProLong™ Diamond Antifade Mountant with DAPI (Invitrogen, Eugene, OR, United States) for staining nucleus, and fluorescence images were obtained by using Leica TCS SP8 confocal microscope. For quantification of LD accumulation, cells were seeded in a 96-well plate and induced adipogenesis differentiation. After washing with PBS, 5 μ L of AdipoRed™ Assay Reagent (Lonza) was added in each well containing 200 μ L PBS and incubated for 10 min at room temperature. Fluorescence with excitation at 485 nm and emission at 572 nm was measured by using a microplate reader (Varioskan LUX).

Microarray Analysis

Total RNA was extracted as above, and 250 ng of RNA was subjected to strand synthesis using GeneChip 3' IVT PLUS Reagent Kit (Affymetrix Inc., Santa Clara, CA, United States) and Affymetrix® 3' IVT Array Strips for GeneAtlas® System (GeneChip® HG-U219) following the manufacturer's protocol. Probe cell intensity values were obtained by GeneAtlas™ Imaging Station; CEL files from probe sets were generated by the Expression Console (Affymetrix) and then analyzed by Transcriptome Analysis Console v4.0 (Affymetrix, Japan) as described previously (Ganbold et al., 2019). We have used three technical replicates of each sample (IN, Sq, and HH-Sq) that represent the same hybridization mixture applied to three independent arrays. Gene expression values refer to Tukey bi-weight average of gene level intensity of all the replicates in a condition. A threshold value of fold change $\geq \pm 1.2$ (in linear space) and $p < 0.05$ [one-way between-subject analysis of variance (ANOVA)] employed by the manufacturer's analysis package was set to identify differentially expressed genes (DEGs). Downstream analyses were conducted using the functional annotation clustering of DAVID Informatics Resources 6.8¹ (Huang et al., 2009), and GSEA's Molecular Signatures Database v7.1² (Subramanian et al., 2005) for gene ontology (GO) and biological process (BP) clustering. GOs with $p < 0.05$ in DAVID (modified Fisher exact test with default EASE score threshold 0.1) were considered as significantly enriched. The microarray dataset was deposited in the NCBI Gene Expression Omnibus (GEO) and is accessible with the accession number GSE153391³.

ATP Assay

ATP production was determined by the "cell" ATP assay luminescent reagent version 2 (CA2-50, Toyo Benet, Japan). Cells were seeded in white clear-bottom 96-well plate, and induced

adipogenesis. After 14 days, according to the manufacturer's protocol, the luminescent reagent (100 μ L/well) was added and followed by 1 min on shaker and 10 min for incubation in dark at room temperature. Luminescence amount (RLU) was measured by microplate reader (Varioskan LUX) and normalized to cell number using Cell Count Normalization kit (Dojindo, Japan).

Mitochondrial Staining by Rhodamine 123

Mitochondrial biogenesis was evaluated by rhodamine 123 assay. Cells were seeded in black clear-bottom 96-well plate and induced adipogenesis. At day 14 (D14), the supernatant was replaced by 50 μ M rhodamine 123 (Wako, Japan) dissolved in Hanks balanced salt solution (Gibco) containing 20 mM HEPES (100 μ L/well) and incubated at 37°C for 30 min. The supernatant was discarded and rinsed with the buffer two times before measuring rhodamine 123 fluorescence intensity [relative fluorescence unit (RFU)] using the excitation/emission at 485/525 nm by microplate reader (Varioskan LUX). RFU was normalized to cell number using Cell Count Normalization kit (Dojindo, Japan). After staining with rhodamine 123, cell nuclei were counterstained with 0.5 μ g/mL Hoechst 33342 (Molecular Probes, United States) dissolved in PBS (100 μ L/well) for 10 min at room temperature for fluorescent imaging using automated inverted microscope (IX83, Olympus).

Glucose Uptake Assay

Glucose uptake was determined by Glucose CII test kit (Wako, Japan). Cells were seeded in 24-well plate and induced adipogenesis for 14 days. Differentiated adipocytes were starved in serum free medium for overnight. Next day, the medium was replaced with Krebs-Ringer-phosphate-HEPES (KRPH) buffer for glucose starvation. After 2 h of incubation, the buffer was replaced by KRPH containing 11 mM glucose with or without 1 nM insulin for 24 h. Glucose level in the supernatant was quantified by colorimetric assay according to the manufacturer's instruction.

Real-Time Reverse Transcription-Polymerase Chain Reaction Analysis

Cells were seeded and induced adipogenesis in a 6-well plate. Total RNA was extracted by using ISOGEN reagent (Nippon Gene, Toyama, Japan) following the manufacturer's instruction. Complementary DNA was synthesized by reverse transcription from 1 μ g of RNA using SuperScript™ IV VILO™ Master Mix (Invitrogen, Carlsbad, CA, United States). The resultant cDNA (100 ng) was then amplified by the predesigned TaqMan® Gene Expression Assay and TaqMan® Gene Expression Master Mix (Applied Biosystems, Carlsbad, CA, United States) on the 7500 Fast Real-Time PCR System. All predesigned primers were purchased from the Applied Biosystems. Gene expression was normalized to *GAPDH* as an endogenous housekeeping gene, and the relative expression level was calculated using the $2^{-\Delta \Delta Ct}$ method ($n = 3$).

¹<https://david.ncifcrf.gov/>

²<https://www.gsea-msigdb.org>

³www.ncbi.nlm.nih.gov/geo

Capillary Immunoassay

Protein level was evaluated using ProteinSimple capillary immunoassay (WesTM, ProteinSimple). dASCs induced adipogenesis in 6-well plate. Total protein was extracted at D14 using radioimmunoprecipitation assay buffer (Sigma-Aldrich, St. Louis, MO, United States) containing protease inhibitor cocktail (P8340, Sigma-Aldrich), and the protein concentration was quantified using 2-D Quant kit (GE Healthcare, Chicago, IL, United States). An equal amount (0.75 $\mu\text{g}/\mu\text{L}$) of protein diluted in sampling buffer (ProteinSimple) were loaded in 12- to 230-kDa, 25-lane plate (ProteinSimple) and run in WES WS3390 instrument following the manufacturer's instruction. Primary antibodies were purchased from Abcam. Anti-rabbit and anti-mouse secondary antibodies of Detection module for chemiluminescence (ProteinSimple) were used. Imaging and peak area were obtained from Compass for SW software (ProteinSimple). Peak areas were normalized to GAPDH as loading control, and relative ratio was calculated compared to IN.

Statistics

All data are shown as the mean \pm SEM unless otherwise mentioned. Statistical analyses were conducted using GraphPad Prism 8.0. All data were assessed for normality (Shapiro–Wilk test) and kurtosis and skewness (D'Agostino–Pearson omnibus test). A one-way ANOVA followed by Dunnett *post hoc* test was performed to compare the treatment groups to the control group, whereas Tukey *post hoc* test was performed to compare among all three groups. Paired *t* test was used for within-group comparison at two different timepoints. A $p < 0.05$ was considered significant.

RESULTS

Sq and HH-Sq Did Not Alter the Proliferative and Migratory Capacity of dASCs

Adipose-derived stem cells derived from T2D donor may have reduced or lost proliferation and migration potential leading to incapacity to differentiate (Pérez et al., 2015; Barbagallo et al., 2017; Vyas et al., 2019). Thus, we checked first if dASCs were maintaining its functions to proliferate and migrate as a sign of multipotent cells. After full confluence, cells in growth medium were subjected to a scratch/wound and then continued with the treatment of 1 μM Sq and HH-Sq for up to 48 h (Figure 1B). Non-treated (NC) cells were observed to migrate toward the cell-free area 12 h after the initiation of the wound and covered greater than 50% after 24 h and completely closed by 48 h. The wound closure rate in each treatment group reached 100% versus NC at the 48-hour time point (Figure 1C). Treatment with Sq and HH-Sq did not interfere with the migratory capacity of dASCs.

Moreover, expansion potential in culture is an important criterion for further use of stem cell source to differentiate into numerous cell lineages. Therefore, the cell proliferation rate of dASCs was evaluated in the presence of different dose of Sq and HH-Sq (Figures 1D,E), and both compounds did not show any inhibitory effect on the dASC proliferation rate until 20 μM of

dose up to 72 h (48 h, $p = 0.179$; 72 h, $p = 0.895$). These results suggest that dASCs still preserve their proliferative and migratory ability, on which the treatment with Sq and HH-Sq did not show any inhibitory effect.

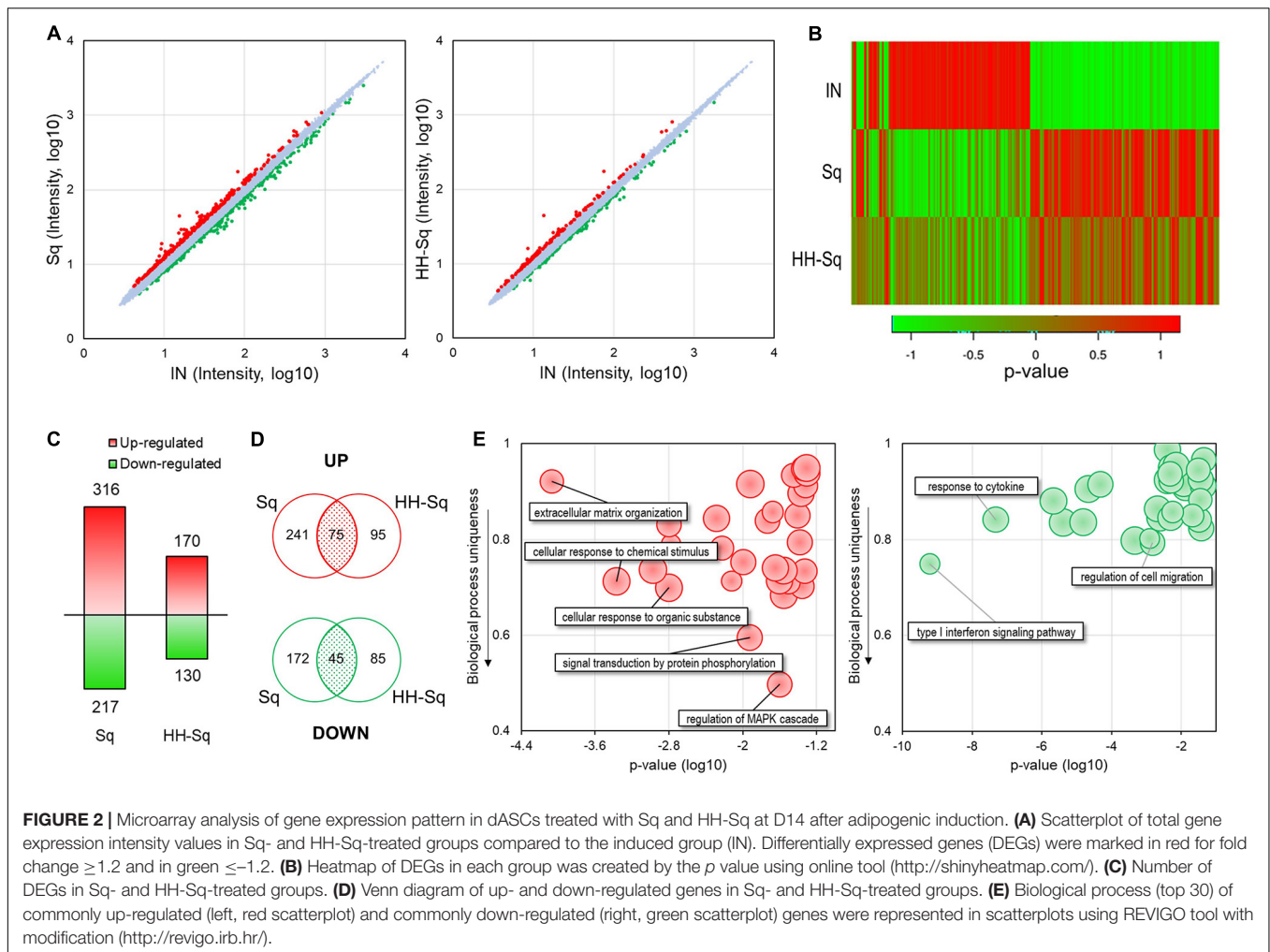
Adipocyte Differentiated From dASCs After Induction

The primary role of stem cells from adipose tissue is to sustain adipocyte turnover by pooling newly differentiated adipocytes. However, evidences showing the capacity of dASCs to differentiate into adipocyte are still controversial (Pérez et al., 2015; Barbagallo et al., 2017). Thus, adipogenesis was induced in dASCs, and the appearance of LDs was observed 7, 14, and 21 days post-induction to explore the differentiation capacity and timing *in vitro* (Figure 1F). Only some of the cells began to show small LD formation at D7. Subsequently, by D14, the number of cells containing LDs occurred increasing along with the enlarged LD size leading the majority of cells engorged with LDs at D21. For further evaluation of the expression of genes, we chose dASCs differentiated on D14 as our model.

Adipocyte-Induced dASCs Gene Expression Pattern Treated With Sq and HH-Sq

Next, we performed microarray analysis using dASCs of D14 after adipocyte differentiation treated with 1 μM Sq and HH-Sq and explored the gene expression profile. Intensity value of total gene probe set after treatment with 1 μM of Sq and HH-Sq compared to the non-treated adipocyte-induced control (IN) is shown (Figure 2A). Probes with a threshold of fold change ≥ 1.2 and $p \leq 0.05$ were considered as DEGs and represented in the heatmap (Figure 2B). In the Sq-treated group, 532 genes were differentially expressed, of which 316 DEGs were up-regulated and 217 DEGs down-regulated, whereas in the HH-Sq-treated group, of 300 DEGs, 170 were up-regulated and 130 were down-regulated (Figure 2C). Subsequently, we analyzed if the respective up- and down-regulated genes in Sq and HH-Sq-treated groups were common or not using Venn diagram (Figure 2D). Interestingly, less than half of the up-regulated genes of HH-Sq (44%) and about one-fourth of Sq (23%) were overlapped, suggesting greater than the majority of genes were up-regulated in a compound-specific way. Similarly, genes overlapping in down-regulation in each group were lower than half of the total number.

Next, we identified main BPs involved in the commonly overexpressed (left, red) and underexpressed (right, green) genes applying GO analysis of DAVID and scattered the most relevant 30 processes according to their p value and uniqueness ratio differing from other BPs (Figure 2E). The most specific BP associated with GO terms mitogen-activated protein kinase (MAPK) cascade regulation (GO:0043408), signal transduction by protein phosphorylation (GO:0023014), and cellular response to chemical stimulus (GO:0070887) were up-regulated by both compounds. Applying the criteria of $p > 0.05$ and containing more than two genes, none of the GO terms among the top 30 BPs involving the common down-regulated genes was specific



to adipogenesis (uniqueness ratio > 0.5), signifying both Sq and HH-Sq do not have any particular common inhibitory effect on the adipogenesis process of dASCs.

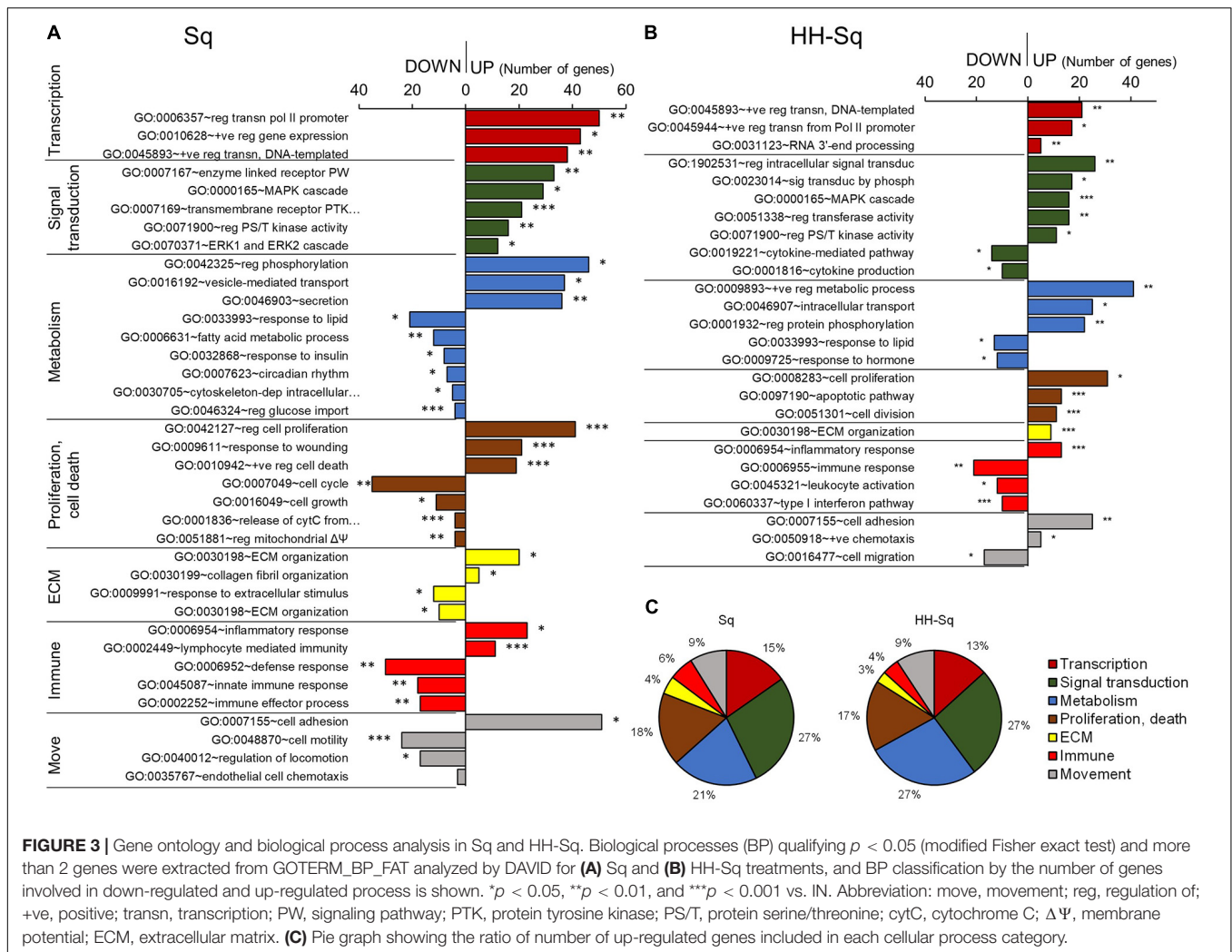
BPs Affected by Sq and HH-Sq Treatment in Adipogenesis of dASCs

Next, to investigate the BP specifically affected by the compound, we identified all BP-qualifying p value greater than 0.05 and containing more than two genes specifically enriched in GO BP FAT terms in Sq and HH-Sq-treated groups and then classified into transcription, signal transduction, metabolism, proliferation and cell death, and extracellular matrix-, immune- and movement-related processes according to their relevance (**Figures 3A,B**). Conversely, large general terms such as regulation of metabolic process (GO:0009893) and regulation of signaling (GO:0023051) were excluded, and terms that are repetitive or similar were merged. Globally, transcriptional activity increased in both treatment groups, as shown by the increased number of genes associated with transcription of polymerase II promoter (GO:0006357) and positive regulation of DNA-templated transcription

(GO:0045893); however, the number of genes enriched was two times higher in Sq group.

Among signal transducing events, MAPK pathway, extracellular signal-regulated protein kinase 1/2 cascade, and serine-threonine kinase activity-related gene expression were increased in Sq followed by cell proliferation regulatory and response to wounding processes activation. These results suggest that the overall MAPK cascade was activated to regulate cell cycle and proliferation during adipogenic differentiation. Hence, metabolic responses, including fatty acid metabolic process (GO:0006631), response to insulin (GO:0032868), and regulation of glucose import (GO:0046324), and cell cycle and growth process were down-regulated.

HH-Sq-treated cells have been found to not only up-regulate similar pathways such as MAPK cascade and serine-threonine kinase activity but also to directly over activates intracellular signal transduction (GO:1902531) and signal transduction by phosphorylation (GO:0023014) compared to Sq-treated cells. In addition, the HH-Sq treatment enhanced positive regulation of metabolic process (GO:0009893) and intracellular transport (GO:0046907). Interestingly, cytokine-mediated pathway (GO:0019221) and cytokine production (GO:0001816) were



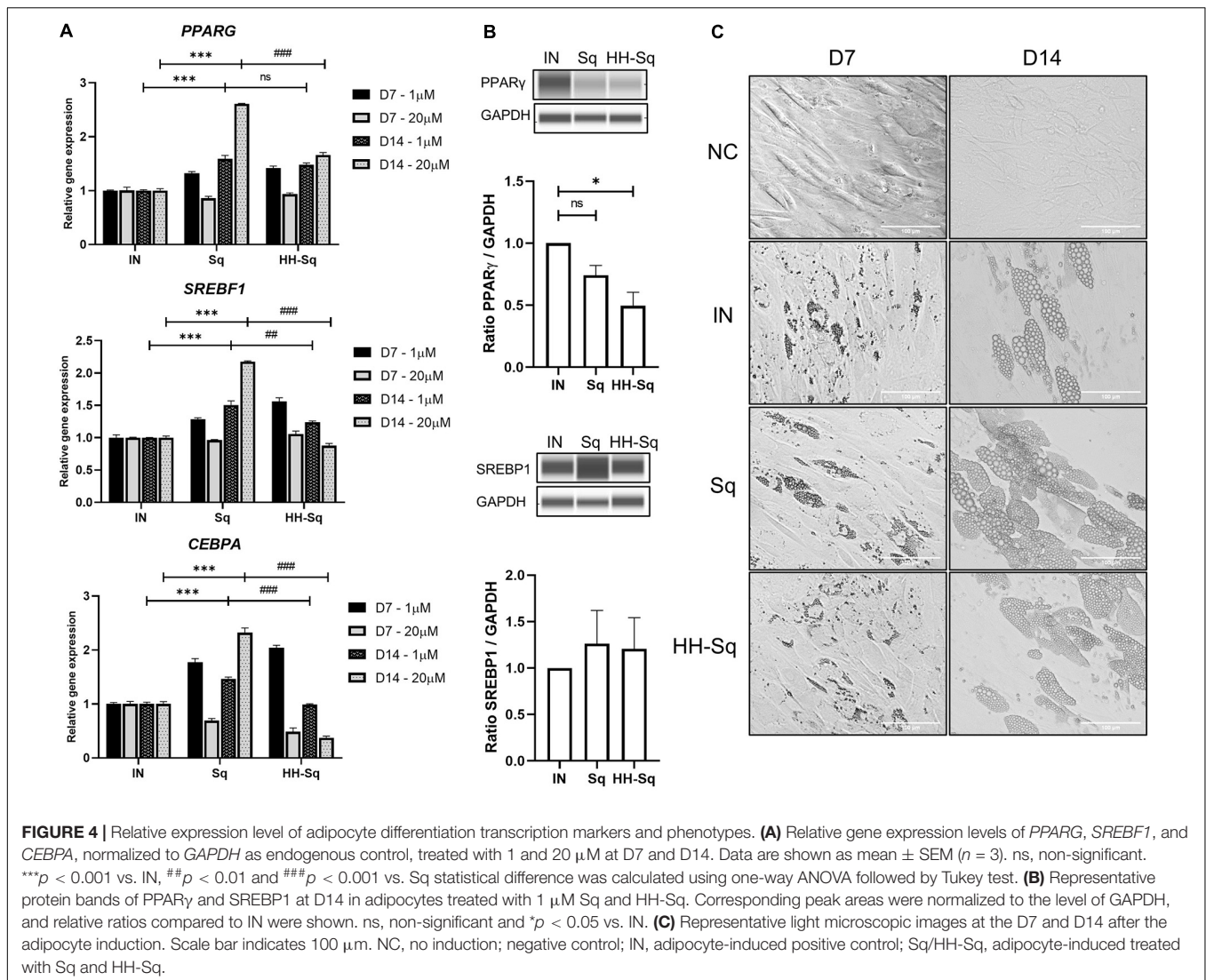
down-regulated, providing another HH-Sq-specific regulation. Inflammatory cytokines secreted by adipocytes in obese and diabetic environment are thought to be increased and promote systemic level of circulating proinflammatory cytokines, thereby contributing to insulin resistance development (Makki et al., 2013; Odegaard and Chawla, 2013). Collectively, the resulting changes show HH-Sq's more favorable effect in alleviating disease-related molecular impairment.

All up-regulated DEGs classified into the cellular processes in Sq and HH-Sq by the number of genes showed a similar ratio suggesting the derivative HH-Sq exerts biological effect, which is comparable to its mother molecule (Figure 3C).

Sq and HH-Sq Promoted Preadipocyte Differentiation Transcription Regulators

Obesity- and diabetes-induced cellular dysfunctions affect adipose tissue-derived stem cell proliferation and differentiation capacity causing reduced turnover in adipocytes, ectopic fat accumulation, and reduced number of preadipocytes (Bost et al., 2005; Van Tienen et al., 2011; Oñate et al., 2012). Thus, we measured gene expression of transcription factors that

control adipogenesis in order to, first, validate the preadipocyte commitment of dASCs, and second, the effect of Sq and HH-Sq on those proadipogenic markers, which direct the differentiation. SREBP1c, peroxisome proliferator-activated receptor γ (PPAR γ), and C/EBP α are early adipogenic markers acting synergistically on the downstream gene expression (Cawthorn et al., 2012). Knockdown of *SREBF1* inhibited adipogenesis and blocked the expression of the other two early markers (Ayala-Sumuano et al., 2011). Consequently, it was found that Sq treatments augmented gene expression of *PPARG*, *SREBF1*, and *CEBPA* compared to non-treated adipocyte-induced control (IN) (Figure 4A). However, the level of these gene expressions in HH-Sq-treated cells except *PPARG* remained inferior to that of Sq treatment, and it decreased in a time- and dose-dependent manner. Protein level of these transcription factors also remained lower in HH-Sq-treated adipocytes (Figure 4B). Of note, the effect of HH-Sq at D7 was comparable to that of Sq at D14 for *PPARG* and *SREBF1* and even higher in *CEBPA*, suggesting there is a temporal shift in the exertion of biological effect between these compounds. General aspect of adipocytes in differentiation at D7 and D14 is shown in Figure 4C. Smaller LDs were found in HH-Sq, whereas



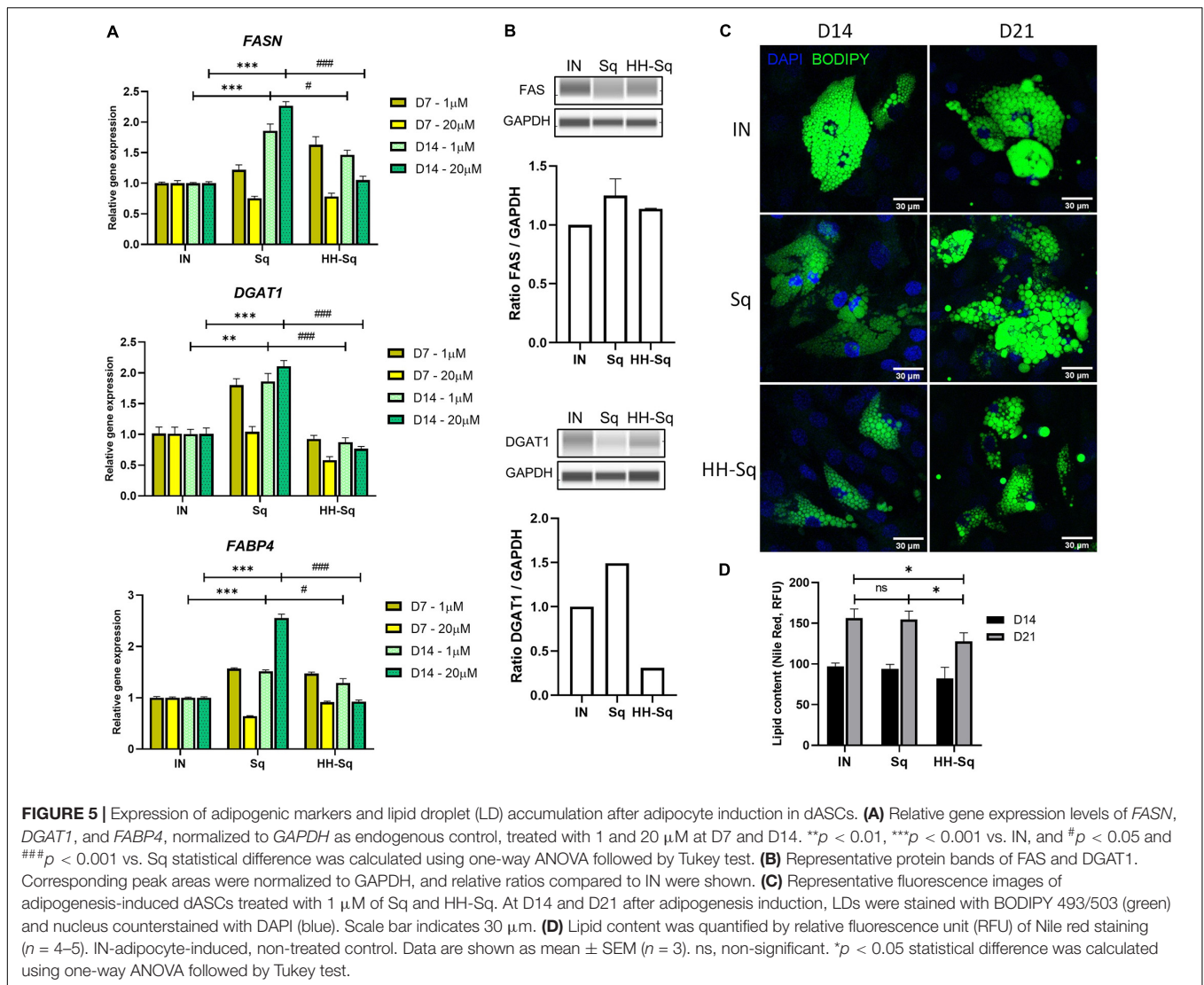
Sq-treated cells showed larger, comparable to IN, droplets that were most likely due to up-regulation of early adipogenic factors.

HH-Sq Induced Adipocytes With Fewer Lipid Droplets

Committed preadipocytes undergo maturation by accumulating LDs as one of their primary roles and expressing subsequent late marker genes of lipogenesis and lipolysis. First, we checked downstream adipocyte-specific gene expression after D7 and D14 (Figure 5A). The fatty acid-binding protein 4 (*FABP4*), also known as adipocyte protein 2), is believed to be expressed in preadipocytes and mature adipocytes and thus required for the maturation of differentiation (Shan et al., 2013). Treatment with Sq and HH-Sq overexpressed *FABP4* compared to IN, showing a similar pattern as early transcription markers; however, increased level in HH-Sq was significantly lower than that in Sq. Next, we measured gene expression of enzymes required for the formation of LDs. Fatty acid synthase (*FASN*) and diacylglycerol acyltransferase (*DGAT1*) are key lipogenic enzymes necessary for

triacylglycerol synthesis and LD formation (Schmid et al., 2005; Harris et al., 2011). Interestingly, both gene expressions were increased after D14 in Sq treatment, whereas only lesser extent for *FASN* not for *DGAT1* by HH-Sq treatment. Corresponding protein levels at D14 showed the similar tendency, however, the difference did not reach statistical significance (Figure 5B). Higher dose seemed to potentiate the effect of compounds, showing more increased expression of these genes by Sq and decreased by HH-Sq.

To extend this result, we observed the effect of treatments on the formation of LD; thus, cells were stained with a dye BODIPY at D14 and D21 after differentiation to visualize intracellular neutral lipids. A large number of newly formed LP appeared in the IN after D14, and its intensity and droplet size became more important by D21 (Figure 5C). Formed LD in Sq-treated cells seemed inferior after D14 of induction, but at D21, cells were engorged with lipids as much as observed in IN, and some cells showed slightly larger LD than IN. By contrast, LD density and size remained evidently fewer and smaller within the



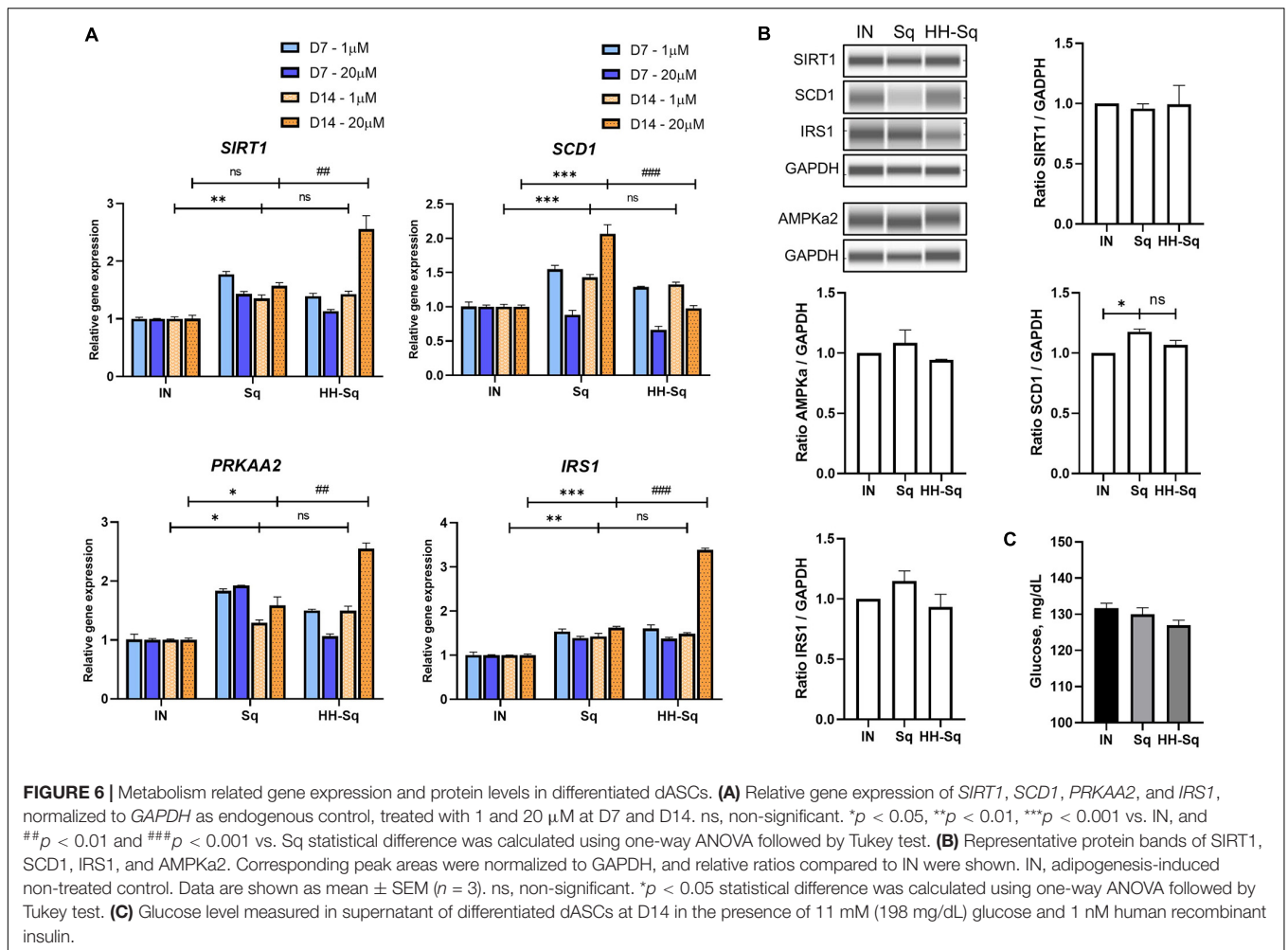
HH-Sq-treated cells. We also assessed the fluorescence intensity of lipids stained with Nile red dye. As observed in microscopic images, lipid content was significantly lower in HH-Sq-treated cells, whereas the lipid intensity was not different in Sq compared to IN up to D21 (Figure 5D). This suggests that the reduced presence of LD in HH-Sq-treated cells is in part due to inhibition of transcription factors but also due to partial inhibition of lipogenic enzymes.

HH-Sq and Sq Increased Expression of Genes Involved in Metabolism

NAD-dependent deacetylase (*SIRT1*), a member of SIRTuins, has been suggested to be down-regulated in insulin-resistant tissue, and its activation improved insulin sensitivity (Sun et al., 2007). In addition, stearoyl-CoA desaturase 1 (*SCD1*), catalyzer in monosaturated fatty acid synthesis, is a key enzyme in *de novo* lipogenesis. Although gene expression of *SIRT1* and *SCD1* showed up-regulation in differentiated adipocytes exposed to 1 μM Sq and HH-Sq, higher concentration (20 μM) of HH-Sq

stimulated the up-regulation of *SIRT1* and down-regulation of *SCD1* by D14, whereas Sq treatment showed the opposite effect (Figure 6A).

AMPK regulates a wide range of metabolic activities and activates *SIRT1* expression and its impairment involved in metabolic syndrome associated pathways (Ruderman et al., 2013). Thus, we measured the expression level of AMP-activated protein kinase (AMPK, gene *PRKAA2*) and insulin receptor substrate 1 (*IRS1*) as important markers of insulin sensitivity. Consistently, *PRKAA2* and *IRS1* genes were found to be overexpressed to the same extent in both treated cells at 1 μM , and this change was highly significant at 20 μM of HH-Sq (Figure 6A). Corresponding protein levels in cells treated at 1 μM were not significant (Figure 6B). After 14 days of adipogenic differentiation, we measured the glucose uptake rate in presence of insulin. The glucose concentration present in the supernatant of HH-Sq was slightly lower than Sq and IN (Figure 6C), suggesting improved glucose uptake. These observations indicate that HH-Sq prevented more effectively



overactivation of lipogenesis, and in turn, more metabolic gene expressions were enhanced.

Mitochondrial Biogenesis Improved by Sq and HH-Sq Treatment

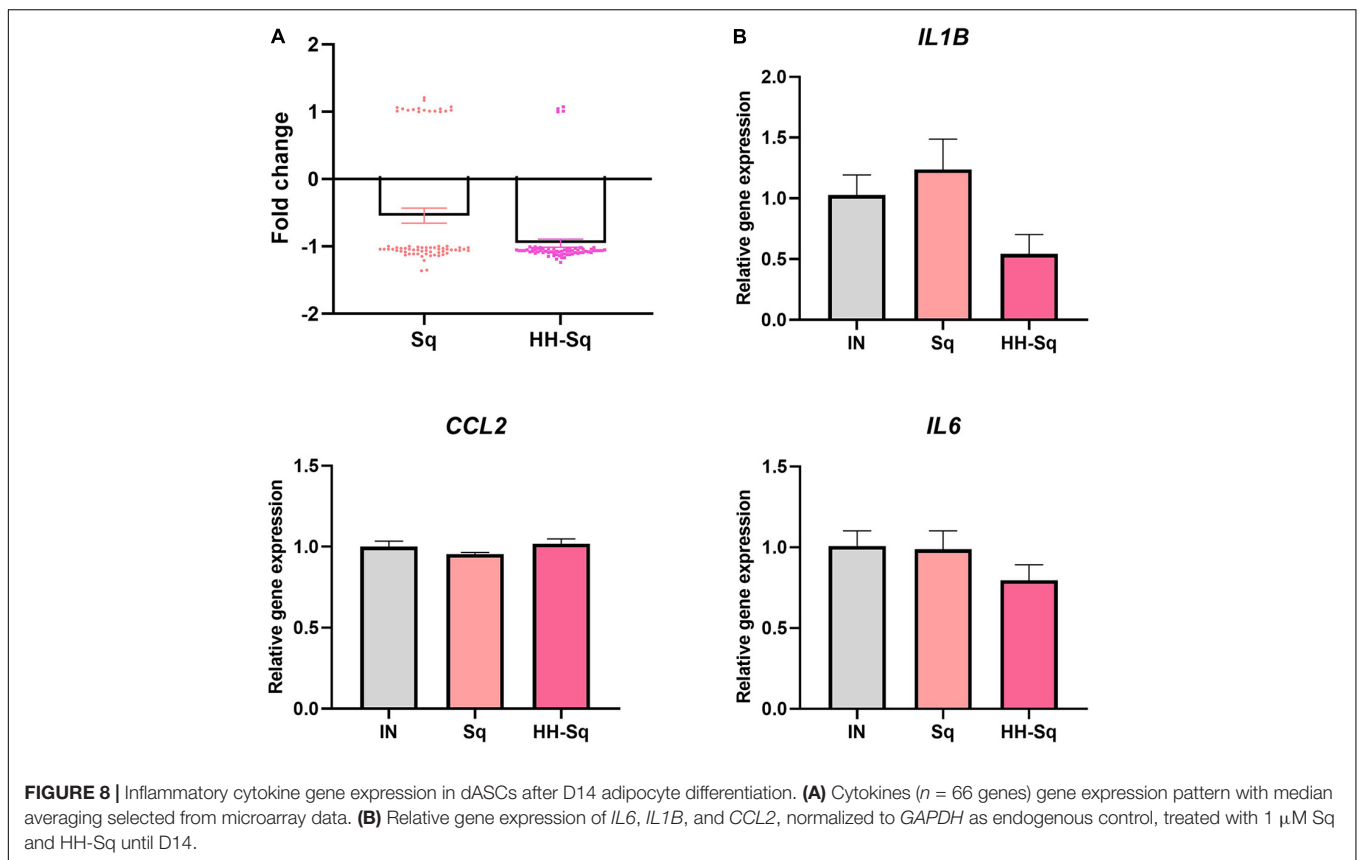
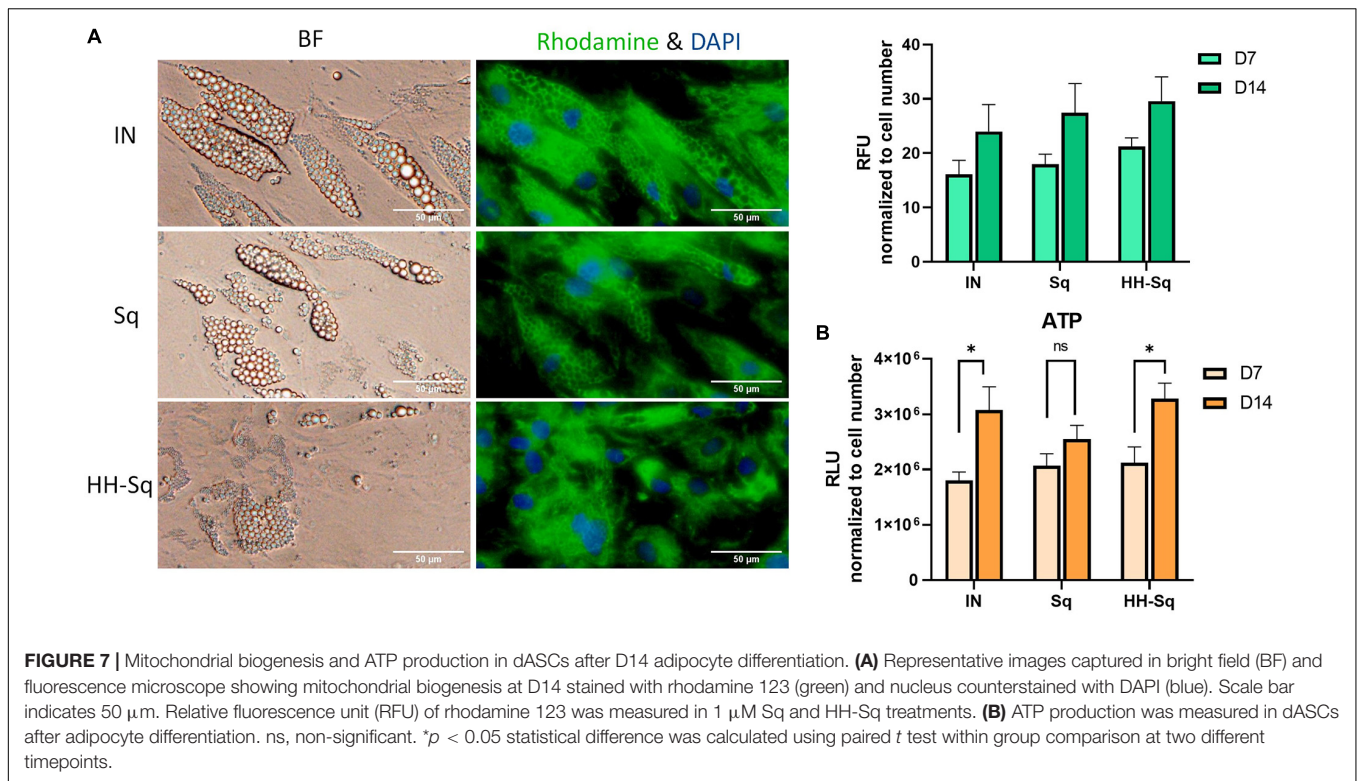
Mitochondria play an important role in energy homeostasis, apoptosis, and inflammation. In adipose tissue, mitochondrial metabolism and function are correlated to adipocyte differentiation, lipid metabolism, and insulin sensitivity (De Pauw et al., 2009). Therefore, mitochondrial dysfunction is widely reported to be implicated in metabolic diseases, obesity, and T2D (McBride et al., 2006; Green et al., 2011). Adipogenic transcription factors contribute in mitochondrial biogenesis during adipogenesis (Spiegelman et al., 2000). Thus, we evaluated mitochondrial biogenesis and ATP production in differentiated adipocytes at D7 and D14. As shown in **Figure 7A**, mitochondrial content increases throughout the adipogenesis from D7 to D14 in all groups. In Sq- and HH-Sq-treated cells, mitochondria remained nevertheless slightly augmented compared to IN. Mitochondrial proliferation in HH-Sq was accompanied by increased ATP production at D14 (**Figure 7B**), suggesting the process of adipogenesis and energy metabolism

were concomitantly stimulated. This finding of mitochondrial content in Sq was not correlated to the level of ATP content, which increased to a lesser extent from D7 to D14.

Mitochondrial biogenesis alteration and its dysfunction are in part attributed to inflammatory or pathologic condition, which further leads to development of metabolic diseases and insulin resistance (Kim et al., 2008). Thus, we sought to analyze the changes in inflammatory cytokines in correlation with the treatment of Sq and HH-Sq during adipogenesis. Cytokine gene expression pattern of microarray data revealed a clear correlation of HH-Sq treatment and the number of down regulated inflammatory cytokines, although both Sq and HH-Sq prevented overexpression of a large number of cytokines (**Figure 8A**; list of genes in **Supplementary Material**). Gene expression levels by quantitative polymerase chain reaction showed slightly ameliorated tendency in HH-Sq-treated cells; however, none of *IL6*, *IL1B*, and *CCL2* reached a statistical significance (**Figure 8B**).

DISCUSSION

Pathogenic fat cells turn against their initial role in organism contributing to metabolic disorders such as obesity, T2D, and



cardiovascular diseases through insulin resistance, an increase of free fatty acids, and impaired adipokines secretion (Van Gaal et al., 2006; Skurk et al., 2007). To compete with old hypertrophied pathogenic adipose tissue (Skurk et al., 2007) emitting undesired biological effects, researchers have been seeking more functional and responsive compounds that can promote new adipocyte differentiation, while not depleting the number of stem cells in reserve (McLaughlin et al., 2007; Ghaben and Scherer, 2019).

Adipose-derived stem cells have the properties of self-renewal and migration (Mazini et al., 2020). ASCs derived from subjects with diabetes showed the similar migratory and proliferative capacity in the absence and presence of Sq and HH-Sq, suggesting that the dASCs maintained the stem cell features, and both compounds exhibited neither depletion of stem cells nor interference on proliferation and migration.

Observations from global microarray data such as up- and down-regulated genes following the treatment with Sq and HH-Sq showed, respectively, different patterns in the number of genes and the process compared to that of commonly regulated genes. Despite this, MAPK cascade and protein serine-threonine kinase activity were commonly up-regulated. MAPK cascade is an important effector activated by extracellular stimuli to induce a long-term cellular response by triggering transcription of genes in the nucleus.

After adipocyte differentiation at D14, various genes involved in transcriptional regulation of adipogenesis differentiation were induced by Sq and HH-Sq treatment. For example, early markers, *PPARG*, *SREBF1*, and *CEBPA*, were overexpressed by Sq and lesser extent by HH-Sq. This ratio was preserved in the downstream lipogenic gene expression. Sq overactivated *FABP4*, *DGAT1*, and *FASN*, whereas their increased level of expression by HH-Sq was significantly lower compared to Sq. Furthermore, the observed effect of HH-Sq was more important at a higher dose. The resulting changes could be observed in LD size and intensity. In HH-Sq-treated adipocytes, the lipogenic genes were down-regulated with the formation of less and smaller LD up to D21 after differentiation.

The role of SCD1 is still controversial. SCD1 deficiency reduced lipogenesis and improved insulin sensitivity in adipose tissue (Flowers and Ntambi, 2008; Ralston and Mutch, 2015); however, SCD1-deficient mice have altered fatty acid re-esterification and glyceroneogenesis in white adipose tissue (Dragos et al., 2017). In Sq- and HH-Sq-treated cells, *SCD1* gene expression was increased but did not show any aberrant lipid accumulation in adipocytes. Hui et al. (2017) reported that mice with adipose tissue specific ablation of *SIRT1* are more susceptible to insulin resistance and argued adipocyte *SIRT1* plays an important role in glucose homeostasis through modulation of macrophages. We observed a significant increase of *SIRT1* in Sq- and HH-Sq-treated adipocytes, which suggests improved glucose homeostasis.

Moreover, studies reported that AMPK is an important sensor of metabolic changes, and its level is highly reduced in insulin-resistant and morbidly obese subjects (Xu et al., 2012; Desjardins and Steinberg, 2018) and is activated in

response to energy metabolism through AMPK-SIRT1-PCG-1 α pathway to enhance mitochondrial oxidative function in adipocytes (Chau et al., 2010). In addition, IRS1 is known as a major insulin receptor substrate in mediating insulin action, and Rondinone et al. (1997) found that the level of IRS1 was significantly reduced in adipocytes of subjects with non-insulin-dependent T2D. Despite increased mitochondrial content both in Sq and HH-Sq indicates the induction of adipogenesis, ATP production level in Sq remained lower by D14. It might be inferred that more ATP was consumed for lipogenesis compared to HH-Sq, which is consistent with the results of overexpressed lipogenic genes followed by Sq treatment. Increased mitochondrial biogenesis and ATP production in HH-Sq-treated cells and the amelioration of glucose uptake in correlation with increased expression of *IRS1* can provide all collectively the benefic effect of HH-Sq in regulation of energy metabolism in adipocytes and its differentiation.

Local inflammatory status in adipose tissue systematically attracts macrophages and leukocytes as well as transforms resident macrophages into an activated form, which collectively aggravates insulin resistance and system inflammation (Chawla et al., 2011; Russo and Lumeng, 2018). Down-regulation of genes related to cytokine production and cytokine-mediated pathway by HH-Sq treatment also suggests that HH-Sq may have an anti-inflammatory effect because low-grade inflammation has been reported being increased in adipocytes of obese subjects due to the proinflammatory cytokines (Lasselien et al., 2014), which affect the pathogenicity of adipocytes (Ghaben and Scherer, 2019). Selected cytokine gene expression data from microarray ($n = 66$ genes) including individual gene expression levels (*IL6*, *IL1B*, and *CCL2*) tended to be ameliorated by HH-Sq treatment, whereas Sq-treated cells were not different than non-treated cells. However, the direct effect on adipocytes was not statistically significant; several protective effects might be stimulated. HH-Sq may improve inflammatory status in systemic level as adipose tissue macrophages are also inflammatory and contribute to adipocyte inflammation. This is supported by Sasaki et al. (2020) findings showing the anti-inflammatory effect of HH-Sq in murine macrophage model.

HH-Sq was synthesized from Sq by adding monoethylene glycol moiety with the aim of improving its hydrophilicity; however, the compounds actually exhibited difference at gene expression level in adipocyte differentiation. In particular, transmembrane receptor protein tyrosine kinase pathway and enzyme-linked receptor pathway genes were enriched by Sq treatment, whereas intracellular signal transduction and transduction by phosphorylation activities were specifically activated by HH-Sq as found by microarray analysis. Furthermore, the effect of HH-Sq on early adipogenic markers seems to precede that of Sq, showing comparable effect at D7 to Sq at D14. This suggests that HH-Sq might have penetrated cell membrane more actively than Sq and exerted its effect faster, which may, in part, explain the increased intracellular signaling genes in HH-Sq-treated cells. Intracellular signaling is necessary for long-term effect at the nucleus level by initiating gene expression, rather than short-term effect in cytoplasmic level.

In contrast, processes related to glucose transport and insulin signaling such as cytoskeleton-dependent intracellular transport (GO:0030705), response to insulin (GO:0032868), regulation of glucose import (GO:0046324), and response to growth factor (GO:0070848) were down-regulated in Sq-treated cells, suggesting Sq does not only weakly reach intracellular environment but also affect insulin signaling effector molecules at probably cell membrane level.

According to the current findings, it could be assumed that both Sq and HH-Sq exert an adipogenic effect on dASCs, and HH-Sq specifically enhances energy metabolism and insulin signaling without aberrantly activating lipogenesis during adipocyte differentiation. Effect of HH-Sq on ASCs derived from altered microenvironment can contribute to the resolution of insulin resistance and obesity-associated metabolic disorders, and the further development of an alternative class of therapeutics derived from a natural compound, and application in tissue engineering of fat. Nevertheless, future research should explore the molecular mechanism by which HH-Sq triggers intracellular signaling.

DATA AVAILABILITY STATEMENT

The datasets presented in this study can be found in online repositories. The names of the repository/repositories and

accession number(s) can be found below: <https://www.ncbi.nlm.nih.gov/>, GSE153391.

AUTHOR CONTRIBUTIONS

MG: conceptualization, methodology, investigation, visualization, validation, and original draft writing. MG and FF: formal analysis and data curation. FF: performed microarray experiment. TA and KT: synthesized HH-Sq. FF, HI, and TA: writing review & editing. KT and HI: supervision and funding acquisition. All authors reviewed the manuscript.

FUNDING

This study was supported by the Japan Science and Technology Agency (JST); Science and Technology Research Partnership for Sustainable Development (SATREPS, Grant No. JPMJSA1506).

SUPPLEMENTARY MATERIAL

The Supplementary Material for this article can be found online at: <https://www.frontiersin.org/articles/10.3389/fcell.2020.577259/full#supplementary-material>

REFERENCES

- Ayala-Sumuano, J. T., Velez-Delvalle, C., Beltrán-Langarica, A., Marsch-Moreno, M., Cerbón-Solorzano, J., and Kuri-Harcuch, W. (2011). Srebf1a is a key regulator of transcriptional control for adipogenesis. *Sci. Rep.* 1, 1–8. doi: 10.1038/srep00178
- Barbagallo, I., Li Volti, G., Galvano, F., Tettamanti, G., Pluchinotta, F. R., Bergante, S., et al. (2017). Diabetic human adipose tissue-derived mesenchymal stem cells fail to differentiate in functional adipocytes. *Exp. Biol. Med.* 242, 1079–1085. doi: 10.1177/1535370216681552
- Bost, F., Aouadi, M., Caron, L., and Binétry, B. (2005). The role of MAPKs in adipocyte differentiation and obesity. *Biochimie* 87, 51–56. doi: 10.1016/j.biochi.2004.10.018
- Cawthorn, W. P., Scheller, E. L., and MacDougald, O. A. (2012). Adipose tissue stem cells meet preadipocyte commitment: going back to the future. *J. Lipid Res.* 53, 227–246. doi: 10.1194/jlr.R021089
- Chau, M. D. L., Gao, J., Yang, Q., Wu, Z., and Gromada, J. (2010). Fibroblast growth factor 21 regulates energy metabolism by activating the AMPK-SIRT1-PGC-1 α pathway. *Proc. Natl. Acad. Sci. U.S.A.* 107, 12553–12558. doi: 10.1073/pnas.1006962107
- Chawla, A., Nguyen, K. D., and Goh, S. Y. P. (2011). Macrophage-mediated inflammation in metabolic disease. *Nat. Rev. Immunol.* 11, 738–749. doi: 10.1038/nri3071
- Costa, M. A., Mangione, M. R., Santonocito, R., Passantino, R., Giacomazza, D., and Librizzi, F. (2018). Biophysical characterization of aolelectin-squalene liposomes. *Colloids Surfaces B Biointerfaces* 170, 479–487. doi: 10.1016/j.colsurfb.2018.06.032
- De Pauw, A., Tejerina, S., Raes, M., Keijer, J., and Arnould, T. (2009). Mitochondrial (dys)function in adipocyte (de)differentiation and systemic metabolic alterations. *Am. J. Pathol.* 175, 927–939. doi: 10.2353/ajpath.2009.081155
- Desjardins, E. M., and Steinberg, G. R. (2018). Emerging role of AMPK in brown and beige adipose tissue (BAT): implications for obesity, insulin resistance, and Type 2 Diabetes. *Curr. Diab. Rep.* 18:80. doi: 10.1007/s11892-018-1049-6
- Dragos, S. M., Bergeron, K. F., Desmarais, F., Suito, K., Wright, D. C., and Mounier, C. (2017). Reduced SCD1 activity alters markers of fatty acid reesterification, glyceroneogenesis, and lipolysis in murine white adipose tissue and 3T3-L1 adipocytes. *Am. J. Physiol. Cell Physiol.* 313, C295–C304. doi: 10.1152/ajpcell.00097.2017
- Flowers, M. T., and Ntambi, J. M. (2008). Role of stearoyl-coenzyme A desaturase in regulating lipid metabolism. *Curr. Opin. Lipidol.* 19, 248–256. doi: 10.1097/MOL.0b013e3282f9b54d.Role
- Ganbold, M., Owada, Y., Ozawa, Y., Shimamoto, Y., Ferdousi, F., and Tominaga, K. (2019). Isorhamnetin alleviates steatosis and fibrosis in mice with nonalcoholic steatohepatitis. *Sci. Rep.* 9:16210. doi: 10.1038/s41598-019-52736-y
- Ghaben, A. L., and Scherer, P. E. (2019). Adipogenesis and metabolic health. *Nat. Rev. Mol. Cell Biol.* 20, 242–258. doi: 10.1038/s41580-018-0093-z
- Green, D. R., Galluzzi, L., and Kroemer, G. (2011). Mitochondria and the autophagy-inflammation-cell death axis in organismal aging. *Science* 333, 1109–1112. doi: 10.1126/science.1201940
- Harris, C. A., Haas, J. T., Streeper, R. S., Stone, S. J., Kumari, M., and Yang, K. (2011). DGAT enzymes are required for triacylglycerol synthesis and lipid droplets in adipocytes. *J. Lipid Res.* 52, 657–667. doi: 10.1194/jlr.M013003
- He, H. P., Cai, Y., Sun, M., and Corke, H. (2002). Extraction and purification of squalene from *Amaranthus* grain. *J. Agric. Food Chem.* 50, 368–372. doi: 10.1021/jf010918p
- Hernández-Pérez, M., Gallego, R. M. R., Alayón, P. J. P., and Hernández, A. B. (1997). Squalene content in livers from deep-sea sharks caught in Canary Island waters Margarita. *Mar. Fresh Water Res.* 48, 573–576. doi: 10.1071/MF97004
- Huang, D. W., Sherman, B. T., and Lempicki, R. A. (2009). Systematic and integrative analysis of large gene lists using DAVID bioinformatics resources. *Nat. Protoc.* 4, 44–57. doi: 10.1038/nprot.2008.211
- Hui, X., Zhang, M., Gu, P., Li, K., Gao, Y., Wu, D., et al. (2017). Adipocyte SIRT1 controls systemic insulin sensitivity by modulating macrophages in adipose tissue. *EMBO Rep.* 18, 645–657. doi: 10.15252/embr.201643184
- Ishida, M., Tatsumi, K., Okumoto, K., and Kaji, H. (2020). Adipose tissue-derived stem cell sheet improves glucose metabolism in obese mice. *Stem Cells Dev.* 29, 488–497. doi: 10.1089/scd.2019.0250

- Kaya, K., Nakazawa, A., Matsuura, H., Honda, D., Inouye, I., and Watanabe, M. M. (2011). Thraustochytrid *aurantiochytrium* sp. 18w-13a accumulates high amounts of squalene. *Biosci. Biotechnol. Biochem.* 75, 2246–2248. doi: 10.1271/bbb.110430
- Kim, J. A., Wei, Y., and Sowers, J. R. (2008). Role of mitochondrial dysfunction in insulin resistance. *Circ. Res.* 102, 401–414. doi: 10.1161/CIRCRESAHA.107.165472
- Kritchevsky, D., Moyer, A. W., and Tesar, W. C. (1953). Squalene feeding in experimental atherosclerosis. *Arch. Biochem. Biophys.* 44, 241–243. doi: 10.1016/0003-9861(53)90029-0
- Lasselun, J., Magne, E., Beau, C., Ledaguenel, P., Dexpert, S., Aubert, A., et al. (2014). Adipose inflammation in obesity: relationship with circulating levels of inflammatory markers and association with surgery-induced weight loss. *J. Clin. Endocrinol. Metab.* 99, 53–61. doi: 10.1210/jc.2013-2673
- Makki, K., Froguel, P., and Wolowczuk, I. (2013). Adipose tissue in obesity-related inflammation and insulin resistance: cells, cytokines, and chemokines. *ISRN Inflamm.* 2013, 1–12. doi: 10.1155/2013/139239
- Mazini, L., Rochette, L., Admou, B., Amal, S., and Malka, G. (2020). Hopes and limits of adipose-derived stem cells (ADSCs) and mesenchymal stem cells (MSCs) in wound healing. *Int. J. Mol. Sci.* 21:1306. doi: 10.3390/ijms21041306
- McBride, H. M., Neuspiel, M., and Wasiak, S. (2006). Mitochondria: more than just a powerhouse. *Curr. Biol.* 16, 551–560. doi: 10.1016/j.cub.2006.06.054
- McLaughlin, T., Sherman, A., Tsao, P., Gonzalez, O., Yee, G., Lamendola, C., et al. (2007). Enhanced proportion of small adipose cells in insulin-resistant vs insulin-sensitive obese individuals implicates impaired adipogenesis. *Diabetologia* 50, 1707–1715. doi: 10.1007/s00125-007-0708-y
- Moon, K. C., Chung, H. Y., Han, S. K., Jeong, S. H., and Dhong, E. S. (2019). Possibility of injecting adipose-derived stromal vascular fraction cells to accelerate microcirculation in ischemic diabetic feet: a pilot study. *Int. J. Stem Cells* 12, 107–113. doi: 10.15283/ijsc18101
- Naderi, N., Combelleck, E. J., Griffin, M., Sedaghati, T., Javed, M., Findlay, M. W., et al. (2017). The regenerative role of adipose-derived stem cells (ADSC) in plastic and reconstructive surgery. *Int. Wound J.* 14, 112–124. doi: 10.1111/iwj.12569
- Naderi, N., Wilde, C., Haque, T., Francis, W., Seifalian, A. M., Thornton, C. A., et al. (2014). Adipogenic differentiation of adiposederived stem cells in 3-dimensional spheroid cultures (microtissue): implications for the reconstructive surgeon. *J. Plast. Reconstr. Aesthetic Surg.* 67, 1726–1734. doi: 10.1016/j.bjps.2014.08.013
- Nie, C., Yang, D., Xu, J., Si, Z., Jin, X., and Zhang, J. (2011). Locally administered Adipose-derived stem cells accelerate wound healing through differentiation and vasculogenesis. *Cell Transplant.* 20, 205–216. doi: 10.3727/096368910X520065
- Odegaard, J. I., and Chawla, A. (2013). Pleiotropic actions of insulin resistance and inflammation in metabolic homeostasis. *Science* 339, 172–177. doi: 10.1126/science.1230721
- Oñate, B., Vilahur, G., Ferrer-Lorente, R., Ybarra, J., Díez-Caballero, A., Ballesta-López, C., et al. (2012). The subcutaneous adipose tissue reservoir of functionally active stem cells is reduced in obese patients. *FASEB J.* 26, 4327–4336. doi: 10.1096/fj.12-207217
- Owen, R. W., Mier, W., Giacosa, A., Hull, W. E., Spiegelhalter, B., and Bartsch, H. (2000). Phenolic compounds and squalene in olive oils: the concentration and antioxidant potential of total phenols, simple phenols, secoiridoids, lignans and squalene. *Food Chem. Toxicol.* 38, 647–659. doi: 10.1016/S0278-6915(00)00061-2
- Pérez, L. M., Bernal, A., De Lucas, B., Martín, N. S., Mastrangelo, A., García, A., et al. (2015). Altered metabolic and stemness capacity of adipose tissue-derived stem cells from obese mouse and human. *PLoS One* 10:e0123397. doi: 10.1371/journal.pone.0123397
- Ralston, J. C., and Mutch, D. M. (2015). SCD1 inhibition during 3T3-L1 adipocyte differentiation remodels triacylglycerol, diacylglycerol and phospholipid fatty acid composition. *Prostaglandins Leukot. Essent. Fat. Acids* 98, 29–37. doi: 10.1016/j.plefa.2015.04.008
- Rao, C. V., Newmark, H. L., and Reddy, B. S. (1998). Chemopreventive effect of squalene on colon cancer. *Carcinogenesis* 19, 287–290. doi: 10.1093/carcin/19.2.287
- Rondinone, C. M., Wang, L. M., Lonnroth, P., Wesslau, C., Pierce, J. H., and Smith, U. (1997). Insulin receptor substrate (IRS) 1 is reduced and IRS-2 is the main docking protein for phosphatidylinositol 3-kinase in adipocytes from subjects with non-insulin-dependent diabetes mellitus. *Proc. Natl. Acad. Sci. U.S.A.* 94, 4171–4175. doi: 10.1073/pnas.94.8.4171
- Ruderman, N. B., Carling, D., Prentki, M., and Cacicedo, J. M. (2013). AMPK, insulin resistance, and the metabolic syndrome. *J. Clin. Invest.* 123, 2764–2772. doi: 10.1172/JCI67227.2764
- Russo, L., and Lumeng, C. N. (2018). Properties and functions of adipose tissue macrophages in obesity. *Immunology* 155, 407–417. doi: 10.1111/imm.13002
- Sasaki, K., Inami, Y., Tominaga, K., Kigoshi, H., Arimura, T., and Isoda, H. (2020). Synthesis of 2-(2-Hydroxyethoxy)-3-hydroxysqualene and characterization of its anti-inflammatory effects. *Biomed Res. Int.* 2020, 1–9. doi: 10.1155/2020/9584567
- Schmid, B., Rippmann, J. F., Tadayyon, M., and Hamilton, B. S. (2005). Inhibition of fatty acid synthase prevents preadipocyte differentiation. *Biochem. Biophys. Res. Commun.* 328, 1073–1082. doi: 10.1016/j.bbrc.2005.01.067
- Shan, T., Liu, W., and Kuang, S. (2013). Fatty acid binding protein 4 expression marks a population of adipocyte progenitors in white and brown adipose tissues. *FASEB J.* 27, 277–287. doi: 10.1096/fj.12-211516
- Shimizu, N., Ito, J., Kato, S., Eitsuka, T., Miyazawa, T., and Nakagawa, K. (2019). Significance of squalene in rice bran oil and perspectives on squalene oxidation. *J. Nutr. Sci. Vitaminol.* 65, S62–S66. doi: 10.3177/jnsv.65.S62
- Skurk, T., Alberti-Huber, C., Herder, C., and Hauner, H. (2007). Relationship between adipocyte size and adipokine expression and secretion. *J. Clin. Endocrinol. Metab.* 92, 1023–1033. doi: 10.1210/jc.2006-1055
- Spiegelman, B., Puijgsver, P., and Wu, Z. (2000). Regulation of adipogenesis and energy balance. *Int. J. Obes.* 24, 8–10.
- Strandberg, T. E., Tilvis, R. S., and Miettinen, T. A. (1990). Metabolic variables of cholesterol during squalene feeding in humans: comparison with cholestyramine treatment. *J. Lipid Res.* 31, 1637–1643.
- Subramanian, A., Tamayo, P., Mootha, V. K., Mukherjee, S., Ebert, B. L., Gillette, M. A., et al. (2005). Gene set enrichment analysis: a knowledge-based approach for interpreting genome-wide expression profiles. *Proc. Natl. Acad. Sci. U.S.A.* 102, 15545–15550. doi: 10.1073/pnas.0506580102
- Sun, C., Zhang, F., Ge, X., Yan, T., Chen, X., Shi, X., et al. (2007). SIRT1 improves insulin sensitivity under insulin-resistant conditions by repressing PTP1B. *Cell Metab.* 6, 307–319. doi: 10.1016/j.cmet.2007.08.014
- Van Gaal, L. F., Mertens, I. L., and De Block, C. E. (2006). Mechanisms linking obesity with cardiovascular disease. *Nature* 444, 875–880. doi: 10.1038/nature05487
- Van Tienen, F. H. J., Van Der Kallen, C. J. H., Lindsey, P. J., Wanders, R. J., Van Greevenbroek, M. M., and Smeets, H. J. M. (2011). Preadipocytes of type 2 diabetes subjects display an intrinsic gene expression profile of decreased differentiation capacity. *Int. J. Obes.* 35, 1154–1164. doi: 10.1038/ijo.2010.275
- Vyas, K. S., Bole, M., Vasconez, H. C., Banuelos, J. M., Martinez-Jorge, J., Tran, N., et al. (2019). Profile of adipose-derived stem cells in obese and lean environments. *Aesthetic Plast. Surg.* 43, 1635–1645. doi: 10.1007/s00266-019-01397-3
- Xu, X. J., Gauthier, M. S., Hess, D. T., Apovian, C. M., Cacicedo, J. M., Gokce, N., et al. (2012). Insulin sensitive and resistant obesity in humans: AMPK activity, oxidative stress, and depot-specific changes in gene expression in adipose tissue. *J. Lipid Res.* 53, 792–801. doi: 10.1194/jlr.P022905
- Yeh, Y. S., Jheng, H. F., Iwase, M., Kim, M., Mohri, S., Kwon, J., et al. (2018). The mevalonate pathway is indispensable for adipocyte survival. *iScience* 9, 175–191. doi: 10.1016/j.isci.2018.10.019
- Yu, S., Cheng, Y., Zhang, L., Yin, Y., Xue, J., Li, B., et al. (2019). Treatment with adipose tissue-derived mesenchymal stem cells exerts anti-diabetic effects, improves long-term complications, and attenuates inflammation in type 2 diabetic rats. *Stem Cell Res. Ther.* 10, 1–18. doi: 10.1186/s13287-019-1474-8

Conflict of Interest: The authors declare that the research was conducted in the absence of any commercial or financial relationships that could be construed as a potential conflict of interest.

Copyright © 2020 Ganbold, Ferdousi, Arimura, Tominaga and Isoda. This is an open-access article distributed under the terms of the Creative Commons Attribution License (CC BY). The use, distribution or reproduction in other forums is permitted, provided the original author(s) and the copyright owner(s) are credited and that the original publication in this journal is cited, in accordance with accepted academic practice. No use, distribution or reproduction is permitted which does not comply with these terms.